sustainability

MDPI

Article

Mechanical Strength of Saline Sandy Soils Stabilized with Alkali-Activated Cements

Hamid Reza Razeghi [1,*], Pooria Ghadir [1] and Akbar A. Javadi [2,*]

[1] School of Civil Engineering, Iran University of Science and Technology, Tehran 1684613114, Iran
[2] Department of Engineering, University of Exeter, Exeter EX4 4QF, UK
* Correspondence: razeghi@iust.ac.ir (H.R.R.); a.a.javadi@exeter.ac.uk (A.A.J.)

Abstract: Saline soils usually cannot satisfy the requirements of engineering projects because of their inappropriate geotechnical properties. For this reason, they have always been known as one of the problematic soils worldwide. Moreover, the lack of access to normal water has intensified the use of saline water resources such as seawater in many construction and mining projects. Although cement stabilization is frequently used to improve the engineering properties of saline soils, Portland cement's usage as a binder is constrained by its negative consequences, particularly on the environment. In this line, the effects of NaCl on the microstructural and mechanical properties of alkali-activated volcanic ash/slag-stabilized sandy soil were investigated in this study. Moreover, the effects of binder type, slag replacement, curing time, curing condition, and NaCl content on the mechanical strength of stabilized soils were examined. In addition, microstructural analyses, including XRD, FTIR, and SEM–EDS mapping tests, were performed to understand the physical and chemical interaction of chloride ions and alkali-activated cements. The results show that alkali-activated slag can be a sustainable alternative to Portland cement for soil stabilization projects in saline environments. The increase in sodium chloride (NaCl) content up to 1 wt.% caused the strength development up to 244% in specimens with 50 and 100 wt.% slag, and adding more NaCl had no significant effect on the strength in all curing conditions. Microstructural investigations showed that the replacement of volcanic ash with slag resulted in the formation of C-S-H and C-A-S-H gels that reduced the porosity of the samples and increased mechanical strength. Furthermore, surface adsorption and chemical encapsulation mechanisms co-occurred in stabilized soil samples containing slag and volcanic ash.

Keywords: Portland cement; volcanic ash; soil stabilization; slag; sodium chloride; curing condition

check for updates

Citation: Razeghi, H.R.; Ghadir, P.; Javadi, A.A. Mechanical Strength of Saline Sandy Soils Stabilized with Alkali-Activated Cements. *Sustainability* **2022**, *14*, 13669. https://doi.org/10.3390/su142013669

Academic Editors: Hosein Naderpour, Masoomeh Mirrashid and Pouyan Fakharian

Received: 9 September 2022
Accepted: 19 October 2022
Published: 21 October 2022

Publisher's Note: MDPI stays neutral with regard to jurisdictional claims in published maps and institutional affiliations.

Copyright: © 2022 by the authors. Licensee MDPI, Basel, Switzerland. This article is an open access article distributed under the terms and conditions of the Creative Commons Attribution (CC BY) license (https://creativecommons.org/licenses/by/4.0/).

1. Introduction

The existence of chloride ions near sea beaches is considered as one of the most expected causes of soil failure in these areas [1,2]. There are many soils that contain sodium chloride (NaCl) in their chemical composition or are affected by sodium chloride due to their proximity to saltwater sources [3–5]. The surface soils usually interact with the atmosphere, resulting in constant changes in water content [2]. Therefore, some of the dissolved salts may precipitate or crystallize as the moisture content decreases, and some of the precipitated salts present as solid particles redissolve as the moisture content increases. Normally, only dissolved salts affect the mechanical properties of the soil, but precipitated salts can be considered as soil particles [2].

In arid/semi-arid regions, water shortage is driving saltwater usage instead of normal water in mining operations [6]. The potentially unnoticed influence of this shift on mine tailing management is one of the consequences of this shift. In this line, it will be necessary to use sustainable binders for stabilization/solidification of mine tailings. Furthermore, soil improvement methods, including deep mixing and jet grouting, are increasingly turning to the usage of seawater to alleviate water stress [7]. However, there is clear evidence that ordinary Portland cement (OPC) may not provide acceptable strength in aggressive environments such

as chloride-saturated environments [8–10]. Chloride anions (Cl^-) react with the aluminate phase of Portland cement to form voluminous Friedel's salt compounds, which cause the dense microstructure of cement to expand and shatter, lowering soil strength over time [11,12]. To study the effects of the soaking Portland slag cement–fly-ash-stabilized soils in a saline environment, the specimens were immersed in 0 to 15 wt.% concentrations of NaCl solution [9]. Increasing NaCl content resulted in the formation of Friedel's salt, which led to a more porous structure with less mechanical strength [9,13]. The effect of various contents of NaCl on the unconfined compressive strength of Portland-cement-stabilized soft soil was studied [14]. The results show that increasing Cl^- content from 1539 mg/kg to 16,000 mg/kg resulted in a mechanical strength reduction of up to 30% [14]. Another study indicated a high salt concentration (10 wt.% to dry soil) declined the mechanical strength of Portland-cement-stabilized clayey soil up to 60% after 28 days of curing [15]. Additoinally, various NaCl contents (0.075 to 15 wt.% to dry soil) declined both the short-term (7 days) and long-term (28 days) mechanical strength of stabilized clayey soil [16]. The influence of sodium chloride on the strength and modulus of elasticity of marine clay was studied [17]. In this research, as the water salinity increased, the mechanical strength of cement- stabilized (lower than 15%) clay samples declined, while the modulus of elasticity remained constant. On the other hand, some previous research showed a positive or neutral effect of NaCl addition on the mechanical strength of cement-stabilized soils [7,18,19]. In a study, geotechnical engineering properties of cement kiln dust (CKD)-stabilized clayey soil with different NaCl contents were investigated [4]. A total of 10 wt.% (to dry weight of the soil) NaCl increased the compressive strength of CKD-stabilized clayey soil by 18.7% and 8% compared with NaCl-free specimens during 7-day and 28-day curing, respectively [4]. In another study, the effects of seawater on the microstructural and mechanical properties of Portland cement jet-grouted coastal clayey soil was investigated [7]. The results reveal that using natural seawater had no undesirable effect on the strength of the clayey soil [7].

Recently, alkali-activated materials have emerged as sustainable alternative binders to Portland cement for soil stabilization [20–24]. Alkali-activated fly-ash-stabilized soil samples had acceptable performance against exposure to NaCl solution (5 wt.%) for 28 days, and the mechanical strength did not change considerably [25]. The unconfined compressive strength of alkali-activated fly-ash-stabilized clayey soil exposed to saline solution with different concentrations of NaCl did not changed considerably [26]. Alkali-activated fly-ash–slag-stabilized sandy soil specimens were soaked in 5 wt.% NaCl solution for different curing times of 30 to 365 days [27]. The unconfined compressive strength reduction was only 8% after 365 days of soaking in NaCl solution [27]. Furthermore, sodium chloride addition (2 wt.% of total solid mass) to the alkali-activated fly ash had no significant effect on silty sand mechanical strength [18].

According to the previous research on the NaCl effect on Portland-cement-stabilized soils, the need for introducing a sustainable binder suitable for torrid and coastal environmental conditions is felt more than ever. On the other hand, the effects of sodium chloride on the microstructural and mechanical characteristics of alkali-activated cement-stabilized soil specimens have not yet been addressed comprehensively. The present study investigated the effects of binder type, slag replacement, curing time, curing condition, and NaCl content on the unconfined compressive strength of stabilized soils. Additionally, microstructural analyses, including XRD, FTIR, and SEM–EDS mapping tests, were performed to understand the physical and chemical interaction of chloride ions and alkali-activated cements.

2. Materials and Methods

2.1. Soil Properties

The studied soil is a non-plastic silty sand, classified as SM using the Unified Soil Classification system [28]. The soil was collected from Astara, Iran, located on the shores of the Caspian Sea. This type of soil has been observed in large areas of the shores of the Caspian Sea, and due to the liquefaction potential of this type of soil, soil stabilization projects are often carried out in this type of soil. As-received soil is known as saline soil, referring to the previous studies [29].

The grain-size distribution curve of the soil was attained through sieve analysis coupled with hydrometer testing conforming to ASTM D422 [30] and ASTM D7928 [31], respectively, as shown in Figure 1. The maximum and minimum index densities and the specific gravity of the soil were ascertained in accordance with ASTM D4253 [32], ASTM D4254 [33], and ASTM D854 [34], respectively, and are listed in Table 1. C_u, C_c, and G_s are uniformity coefficient, gradation (curvature) coefficient, and specific gravity of the soil, respectively. Using the calculation method in the literature [35], the soil particle size, particle gradation curve, and porosity can be well simulated. The soil porosity and particle size have a direct relationship and, in the process of soil formation, some uneven aggregation of particles with different particle sizes will be formed, resulting in large differences in the soil density.

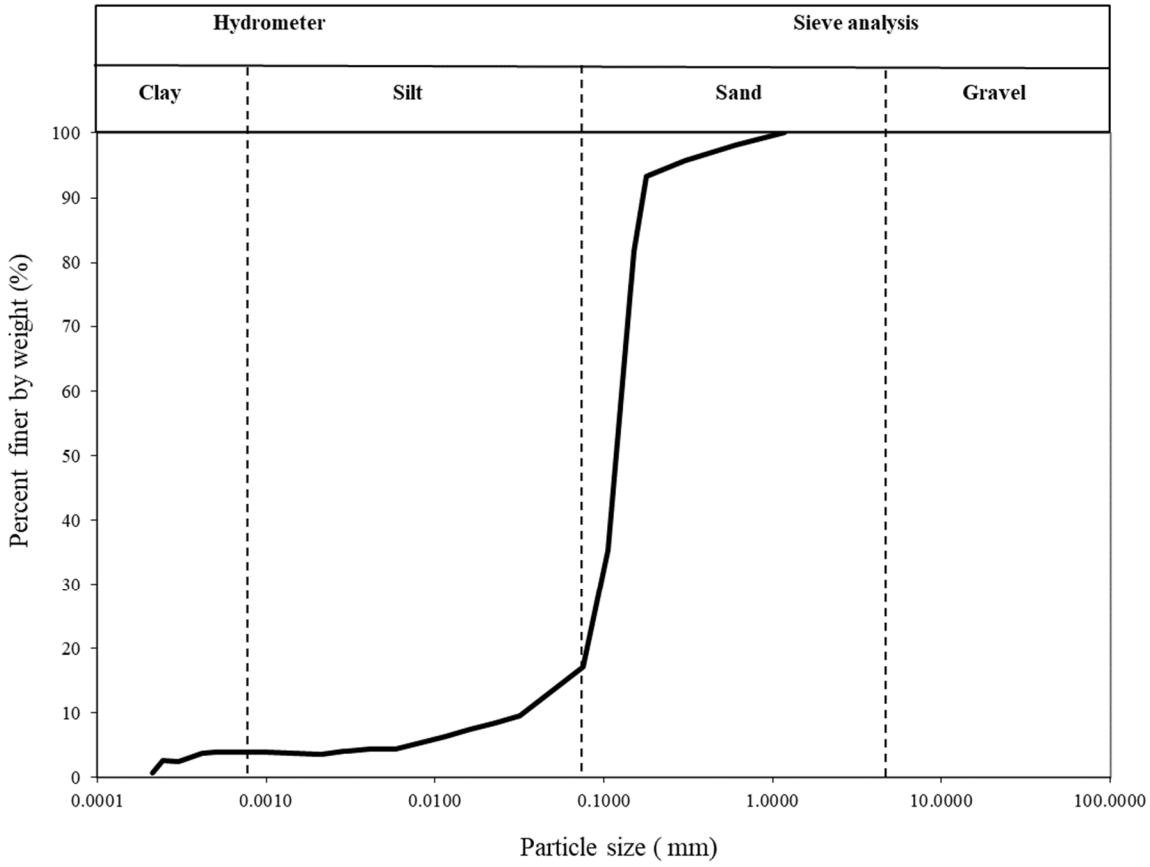

Figure 1. Particle size distribution of the soil.

Table 1. Geotechnical properties of the soil.

Soil Classification	Grain Fractions (%)			D_{10} (μm)	D_{30} (μm)	D_{60} (μm)	C_u	C_c	G_s	γ_{d-max} (kN/m^3)	γ_{d-min} (kN/m^3)
	Clay	Silt	Sand								
SM	4	13	83	37.6	99.8	132.7	3.52	1.99	2.66	16	12.5

2.2. Characterization of Microstructure

The laser diffractometry test was performed using a Mastersizer 3000E (Malvern Panalytical company, United Kingdom).

The chemical compositions of the soil and binders were determined using an X-ray fluorescence (XRF) spectroscope (Axios, Malvern Panalytical company, United Kingdom). All microstructural analyses were carried out on 90-day-cured stabilized soil specimens.

X-Ray diffraction (XRD) pattern measurement was performed using a Bruker company device with a step size of 0.04° and a scanning rate of 0.15° s^{-1} in the 2θ range of 10–90°. XRD analysis was performed using X'PERT HighScore Plus (version 3.0.5) software.

To determine the functional groups, Fourier transform infrared (FTIR) spectroscopy was performed using a Spectrum RXI spectrophotometer in the wave number range of 450–4400 cm^{-1}.

The FEI ESEM QUANTA 200 instrument equipped by elemental mapping spectroscopy (EDS Silicon Drift 2017, RAYSPEC company, Buckinghamshire, UK) was utilized in order to perform scanning electron test.

2.3. Binders and Alkali Activator Characterization

The binders used were Portland cement (OPC-type II), ground-granulated blast furnace slag (slag), and volcanic ash (VA). The OPC, slag, and volcanic ash were supplied by Tehran Cement Company (Tehran, Iran), Sepahan Cement Company (Isfahan, Iran), and Zabol Cement Industries Company (Zabol, Iran), respectively. X-ray fluorescence (XRF) was used to examine the OPC, slag, VA, and soil chemical compositions, Table 2. The laser diffractometry technique was used to investigate the OPC, slag, and VA particle size distributions, shown in Figure 2. XRD patterns of the OPC, slag, VA, and soil is shown in Figure 3. The XRD results indicate that the main mineralogical composition of the soil was quartz, Figure 3.

Table 2. Chemical compositions of VA, slag, OPC, and soil.

Oxide Composition	SiO_2	CaO	Al_2O_3	Fe_2O_3	K_2O	Na_2O	MgO	TiO_2	SrO	SO_3	P_2O_5	MnO	L.O.I
VA [wt.%]	53.89	8.96	20.31	3.44	1.91	5.15	1.42	0.50	0.07	0.26	0.22	-	3.79
Slag [wt.%]	34.86	36.59	13.93	0.20	1.01	-	6.04	1.91	0.08	2.70	-	1.45	1.19
OPC [wt.%]	18.42	61.46	5.23	3.60	0.88	-	2.73	0.36	0.09	4.10	-	0.19	2.90
Soil [wt.%]	45.87	15.52	15.54	6.13	2.04	4.17	2.88	0.63	0.1	0.35	0.24	0.12	9.30

L.O.I = Loss on ignition.

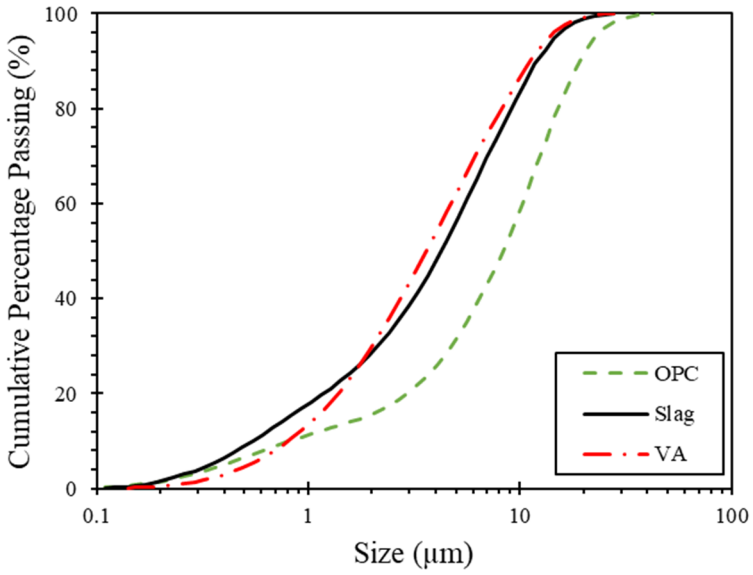

Figure 2. Particle size distributions of OPC, slag, and VA.

Laboratory-grade sodium hydroxide (Merck company with 99% purity) and distilled water were used to prepare the alkaline activator solution.

The NaCl powder (Merck company-CAS number: 1.06404.1000) used in this research had a purity of 99.5%.

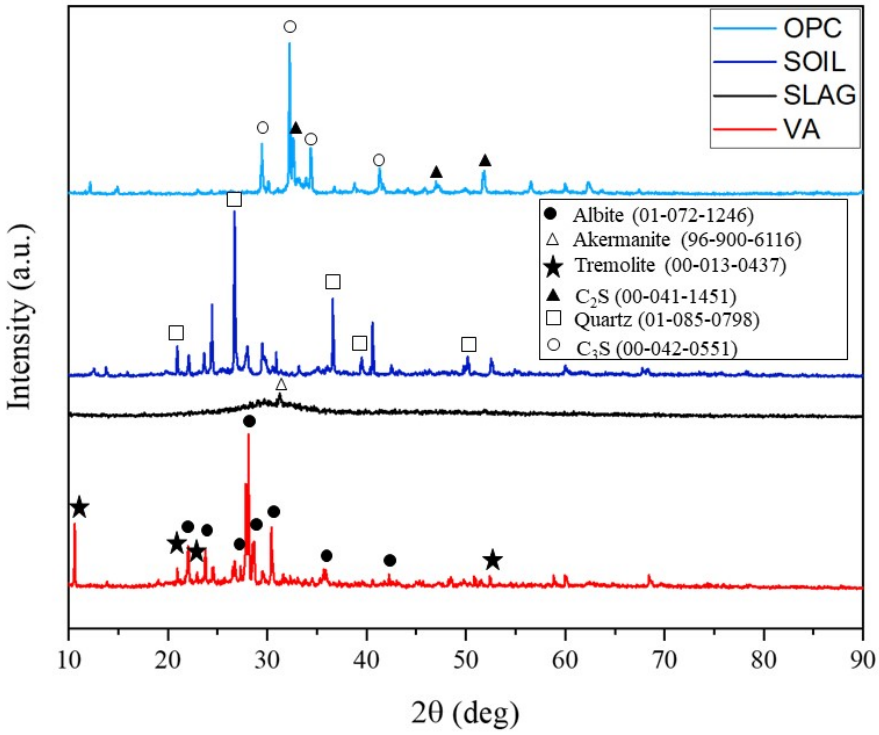

Figure 3. XRD patterns of OPC, slag, VA, and soil.

2.4. Sample Preparation

In order to evaluate the effect of NaCl content on alkali-activated/Portland-cement-stabilized sandy soil, predetermined values of VA/slag were mixed with the activator for a fixed time of 5 min. Sodium hydroxide solution (8 M) and distilled water were used as liquid parts for alkali-activated and Portland cement specimens, respectively. Set 1 was determined to compare the different VA replacement by the slag in the range of 0, 50, and 100 wt.% in alkali-activated specimens. Set 2 was performed on Portland-cement-stabilized sandy soil samples as reference specimens.

A constant binder/soil ratio of 0.3 (mass ratio) was used for all the specimens. To prepare the alkali-activated or Portland cement slurry, predetermined concentrations of binders were mixed with a constant activator/binder ratio of 1 (mass ratio) for 5 min through hand mixing. The soil was manually mixed with 10 wt.% (the weight of soil) distilled water, initial water, and then mixed with alkali-activated or Portland cement slurry for 10 min to reach a uniform mixture. Summary of the mixture proportion is shown in Table 3. To investigate the effect of sodium chloride on mechanical properties of stabilized soils, NaCl was mixed with initial water (0, 1, 2, and 4 wt.% of water). Cylindrical molds (diameter = 38 mm and height = 76 mm) were used to prepare the soil–slurry mixture specimens for the mechanical strength test. The mixture was densified for 60 s using a plate vibrator. In the next step, the molds were placed in a fiberglass chamber with a constant temperature of 25 °C and relative humidity (RH) of 95% for 24 h. In the final stage, specimens were removed from molds and cured at three curing conditions for curing ages of 28 and 90 days. The test plan is shown in Table 4.

Table 3. Mixture proportion of stabilized soil specimens.

Series	Binder Type	Activator Type	Binder/Soil	Activator/Binder	Initial Water (wt.% of Soil)
Alkali-activated	VA/Slag	NaOH (8 M)	0.3	1	10
Portland cement	OPC	H_2O	0.3	1	10

Table 4. Summary of the test plan.

Material Sets	Binder Type	Slag Replacement (%)	Curing Time [day]	Curing Condition	NaCl Content (wt.%)
Set 1	Alkali-activated	0, 50, 100	28, 90	DC *, OC ¥, SC ђ	0, 1, 2, 4
Set 2	OPC	_	28, 90	DC, OC, SC	0, 1, 2, 4

* DC: temperature = 50 °C, relative humidity = 15%; ¥ OC: temperature = 25 °C, relative humidity = 95%; ђ SC: temperature = 25 °C, relative humidity = soaked in distilled water.

2.5. Unconfined Compressive Strength (UCS) Test

According to ASTM D2166 [36], the unconfined compressive strength of stabilized soil specimens was measured with a universal testing machine (Maximum capacity = 50 kN) and a fixed strain rate (1 mm/min). The average of the three measured compressive strengths was recorded as a result of each mechanical strength measurement. A sample of failure mechanism of UCS test is shown in Figure 4.

Figure 4. A sample of failure mechanism of UCS test.

3. Results

3.1. Unconfined Compressive Strength (UCS) Tests

3.1.1. DC Condition

The effect of sodium chloride content and curing time on the mechanical properties of stabilized saline sandy soils at DC condition is shown in Figure 5.

As can be seen, replacing the volcanic ash with 0–100 wt.% slag increased the mechanical strength of the samples at all sodium chloride levels, Figure 5a–c.

A sufficient amount of silicon and calcium for geopolymerization reactions was provided by combining volcanic ash, which is a source of silica, alumina, and slag, which is a source of calcium [37,38]. Subsequently, the amorphous calcium, aluminum, and silicon in volcanic ash and slag were dissolved by the activator, forming monomers with the sodium existing in the alkali activator [39]. The polycondensation of these monomers resulted in the formation of a geopolymer network; the geopolymer network developed within the soil structure and consequently led to improved soil compressive strength [40].

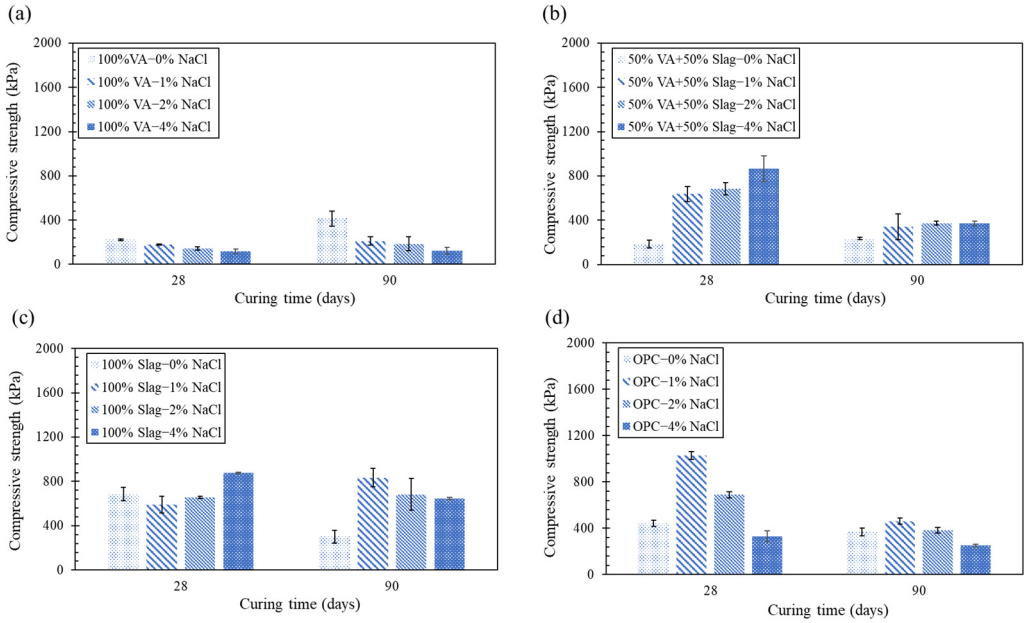

Figure 5. Effect of NaCl content and curing time on the mechanical properties of (**a**) alkali-activated volcanic ash, (**b**) alkali-activated volcanic ash and slag, (**c**) alkali-activated slag, and (**d**) Portland-cement-stabilized saline sandy soils at DC condition.

The strength of samples containing 100% volcanic ash under DC condition gradually increased over time, as shown in Figure 5a. The reason for the strength development might be attributed to the role of water in the geopolymerization process. Structural water is an essentially necessary water for the geopolymerization process and does not evaporate at low temperatures [41,42]. On the other hand, residual water is another type of water in the system which has a negative effect on mechanical properties of specimens. Because of diluting the geopolymer matrix, the speed of the geopolymerization process in both dissolution and hydrolysis stages declined [43,44]. The rheological properties of cementitious systems are modified by the residual water in the system [45–47]. At DC condition, the residual water in the sample structure evaporated and increased the alkalinity of the matrix. In other words, leaching Si and Al was more convenient at the DC condition, and thus the formation speed of geopolymer gel phases was increased [38].

In alkali-activated stabilized soil samples with 50 and 100 wt.% slag, the strength of the samples declined over time. Curing at high temperature without the presence of moisture caused the transfer of moisture from inside to the sample surface, and then it evaporated. This phenomenon caused rapid dehydration and fine crack formation (dry shrinkage) inside the sample [48]. On the other hand, since slag particles undergo both hydration and pozzolanic reactions, when the amount of slag in the sample increased, the need for water increased. Since this amount of water was not supplied, most slag particles remained unreacted. In other words, insufficient alkali activator led to a cessation of pozzolanic reactions. Therefore, unreacted slag particles were placed between soil particles and created porous structure in soil specimens.

As predicted, Portland cement hydration stopped at the DC condition, leading to a reduction in mechanical strength during the 90-day curing period compared with the 28-day curing period, as shown in Figure 5d.

Increasing sodium chloride content from 0 to 4 wt.% in alkali-activated volcanic-ash-stabilized samples led to a gradual reduction in both short-term (28 days) and long-term (90 days) curing periods. With the 50 wt.% slag replacement in the aluminosilicate precursor, the mechanical strength increased steadily with the sodium chloride addition during the short curing period. However, the sodium chloride addition from 0 to 1 wt.% led to an increase in long-term strength, and further sodium chloride addition had no appreciable im-

pact on mechanical strength. By replacing volcanic ash with slag completely, the mechanical strength decreased in the short curing period by increasing the sodium chloride content from 0 to 1 wt.%. By further sodium chloride addition, the short-term mechanical strength increased. In the long curing time, the sodium chloride addition from 0 to 1 wt.% led to an increase in mechanical properties, and further addition of sodium chloride resulted in mechanical strength reduction.

The strength of the Portland-cement-stabilized soil samples rose when the sodium chloride content was increased from 0 to 1 wt.% in the short- and long-term curing periods. However, the strength was reduced when the sodium chloride concentration was raised up to 4 wt.%.

Dissolution of large amounts of chloride ions prevented the completion of the hydration process of Portland cement, resulting in the formation of less C-S-H gel and, ultimately, the reduction in strength of cement specimens [49]. Furthermore, the aluminate phases of Portland cement (tricalcium aluminate (3 $CaO{\cdot}Al_2O_3$) or C_3A) reacted with chloride ions to form Friedel's salt ($C_3A.\ CaCl_2{\cdot}10H_2O$) [50–54]. Friedel's salt formation led to portlandite ($Ca(OH)_2$) phase instability. The formation of such salts can cause the cement paste to set earlier through ettringite deposition, but at the same time, it can damage the cement structure [50–54]. Similar results were observed in previous studies [9,13]. Friedel's salt formed as the NaCl level rose, resulting in a porous structure with reduced mechanical strength [9,13]. The impact of varying NaCl contents on the unconfined compressive strength of soft soil stabilized by Portland cement was investigated [14]. The findings demonstrated that a mechanical strength loss of up to 30% occurred when the Cl-concentration was increased from 1539 mg/kg to 16,000 mg/kg [14]. Another study found that clayey soil stabilized with Portland cement decreased in mechanical strength by up to 60% after 28 days of curing when exposed to high salt concentrations (10 wt.% to dry soil) [15]. Additionally, different NaCl levels (0.075 to 15 wt.% to dry soil) decreased the mechanical strength of stabilized clayey soil over the course of both a short-term (7 days) and long-term (28 days) period [16].

3.1.2. OC Condition

Figure 6 indicates the effect of sodium chloride content and curing time on the mechanical properties of stabilized saline sandy soils at the OC condition.

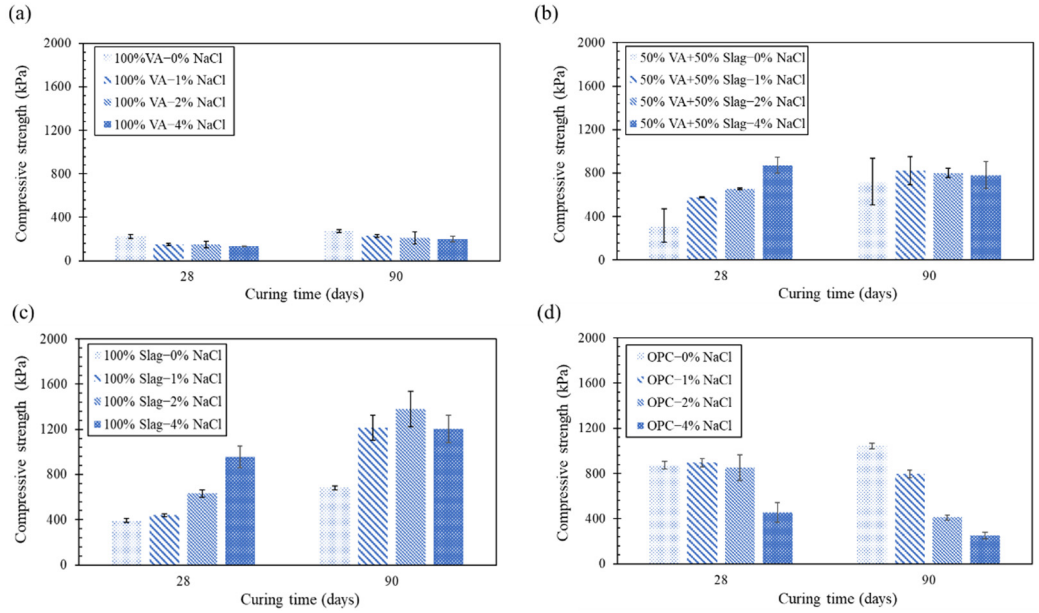

Figure 6. Effect of NaCl content and curing time on the mechanical properties of (**a**) alkali-activated volcanic ash, (**b**) alkali-activated volcanic ash and slag, (**c**) alkali-activated slag, and (**d**) Portland-cement-stabilized saline sandy soils at OC condition.

At the OC conditions similar to the DC condition, the samples' compressive strength was enhanced by adding slag (Figure 6a–c). The strength of samples containing 100 wt.% volcanic ash under the OC condition remained essentially unchanged over time because, unlike the DC condition, the residual water remained in the sample structure, and the alkalinity of the geopolymer matrix did not increase. As a result, the strength of the samples remained almost constant over time.

In alkali-activated stabilized soil samples with 50 and 100 wt.% slag, the strength of the samples generally increased over the curing time. This is because the presence of moisture helps accelerate the slag particles' hydration and pozzolanic reactions, which increases the strength of the slag-containing samples over time.

Wet curing condition also contributed to the Portland cement hydration, and the mechanical strength of Portland-cement-stabilized soil increased over time. However, the addition of sodium chloride prevented strength development in the long curing period.

When sodium chloride content was increased from 0 to 4 wt.% in alkali-activated stabilized soil samples with 100 wt.% volcanic ash across short-term and long-term curing periods, the mechanical strength of the samples gradually declined. Meanwhile, the long-term strength of the samples in alkali-activated stabilized soil samples with 50 and 100 wt.% slag increased with the sodium chloride addition from 0 to 1 wt.%, and the strength of the samples was nearly constant with further sodium chloride addition. With the addition of sodium chloride from 0 to 4 wt.%, the strength of the 90-day Portland-cement-stabilized soil displayed a falling trend, as shown in Figure 6d.

3.1.3. SC Condition

Figure 7 demonstrates the effect of sodium chloride content and curing time on the mechanical properties of stabilized saline sandy soils at SC condition.

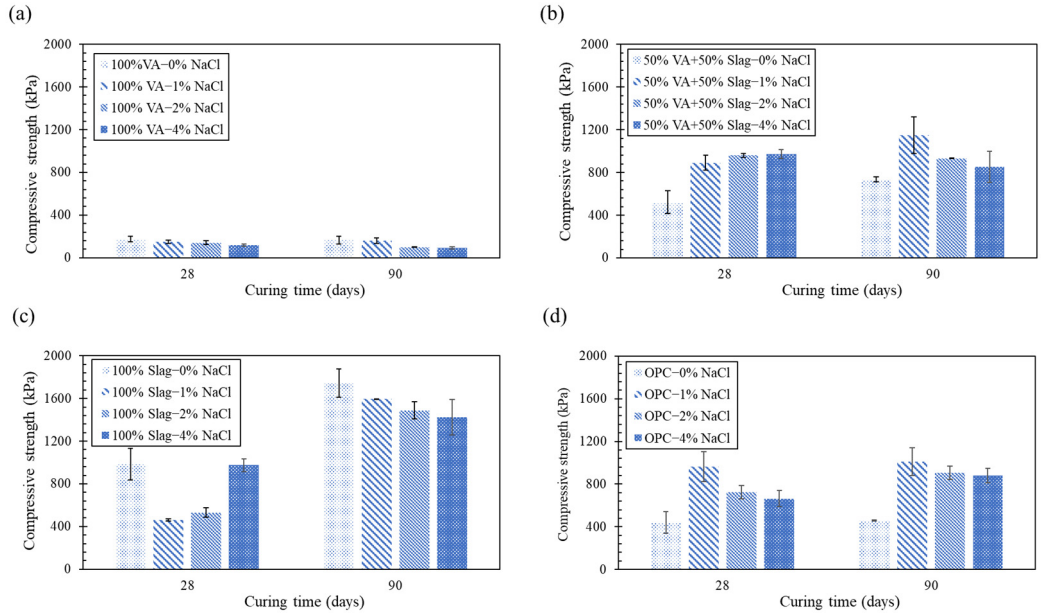

Figure 7. Effect of NaCl content and curing time on the mechanical properties of (**a**) alkali-activated volcanic ash, (**b**) alkali-activated volcanic ash and slag, (**c**) alkali-activated slag, and (**d**) Portland-cement-stabilized saline sandy soils at SC condition.

The rate of slag particles hydration in the presence of water is very slow, so an alkaline activator is usually used to activate the slag particles [55]. In saturated curing conditions, the addition of slag to the samples increases strength (Figure 7a–c).

At the SC condition, the strength of samples containing 100 wt.% volcanic ash decreased over time because in the submerged condition, the activator alkalinity decreased due to the leaching in water, and as a result, the geopolymerization process occurred slowly [27].

In other words, the geopolymer gel dissolved in water to some extent during immersion, which led to a decrease in soil strength [37,38].

In alkali-activated stabilized soil samples with 50 and 100 wt.% slag, the mechanical strength of the samples generally increased over the curing time. This is because the presence of water helps to accelerate the hydration reactions of the slag particles, which in turn increases the strength of the slag-containing samples over time. In other words, the leaching of calcium from stabilizers in the presence of OH^-, Ca^{2+}, AlO_6, and SiO_4 leads to the formation of C-S-H gel, and thus enhances mechanical strength [56]. These reactions continue as long as calcium remains available in the precursors. Hence, the simultaneous presence of C-S-H gel with geopolymerization-induced N-A-S-H gel contributes significantly to soil strength development [57].

Soil submergence can be one of the worst-case scenarios for stabilized soils [38] because the empty voids of the soil are filled with water, and there is a significant reduction in surface tensile forces, which reduces the compressive strength of the soil. According to the obtained results, the use of slag can be considered a promising alternative for the Portland cement in soil stabilization projects.

Submerged curing conditions (SC condition), such as the wet condition (OC condition), contributed to the hydration reaction of cement particles and increased mechanical strength over time. However, the addition of sodium chloride prevented the strength development in the long curing time.

When sodium chloride content was increased from 0 to 4 wt.% in alkali-activated stabilized soil samples with 100 wt.% volcanic ash (Figure 7a), during both short-term and long-term curing periods, the mechanical strength of the samples declined progressively. The long-term strength of the alkali-activated stabilized soil samples with 50 wt.% increased with the sodium chloride addition from 0 to 1 wt.%, and the strength experienced a nuance drop with the further addition of sodium chloride. When sodium chloride was added to alkali-activated stabilized soil samples with 100 wt.% slag in amounts ranging from 0 to 4 wt.%, the samples' long-term strength remained essentially constant. The 90-day strength of the sandy soil stabilized with Portland cement rose with the addition of sodium chloride up to 1 wt.%, while the strength remained essentially unchanged when sodium chloride increased up to 4 wt.%.

3.1.4. The Effect of Curing Condition on UCS

Figure 8 shows the effect of sodium chloride content on mechanical properties (90-day curing) of alkali-activated and Portland-cement-stabilized soil specimens at DC, OC, and SC conditions.

The addition of sodium chloride from 0 to 4 wt.% in the alkali-activated stabilized soil samples with 100 wt.% volcanic ash reduced the strength in all three curing conditions. While in alkali-activated stabilized soil samples with 50 and 100 wt.% slag, with increasing the sodium chloride content, the strength of the samples increased to a certain amount and then remained almost constant in all curing conditions. In SC-cured Portland-cement-stabilized soil samples, with the addition of sodium chloride from 0 to 1 wt.%, the mechanical properties increased, and further addition of sodium chloride up to 4 wt.% had no significant effect on strength. While at both DC and OC conditions, with the addition of sodium chloride from 0 to 4 wt.%, Portland-cement-stabilized samples showed a declining trend.

In all three curing conditions, alkali-activated slag-stabilized soil samples had the highest mechanical strength compared with other stabilized soil samples. Additionally, stabilized soil samples with 50 wt.% slag and Portland-cement-stabilized soil samples had approximately the same strength. Samples containing 100 wt.% volcanic ash had the lowest mechanical strength compared with other samples.

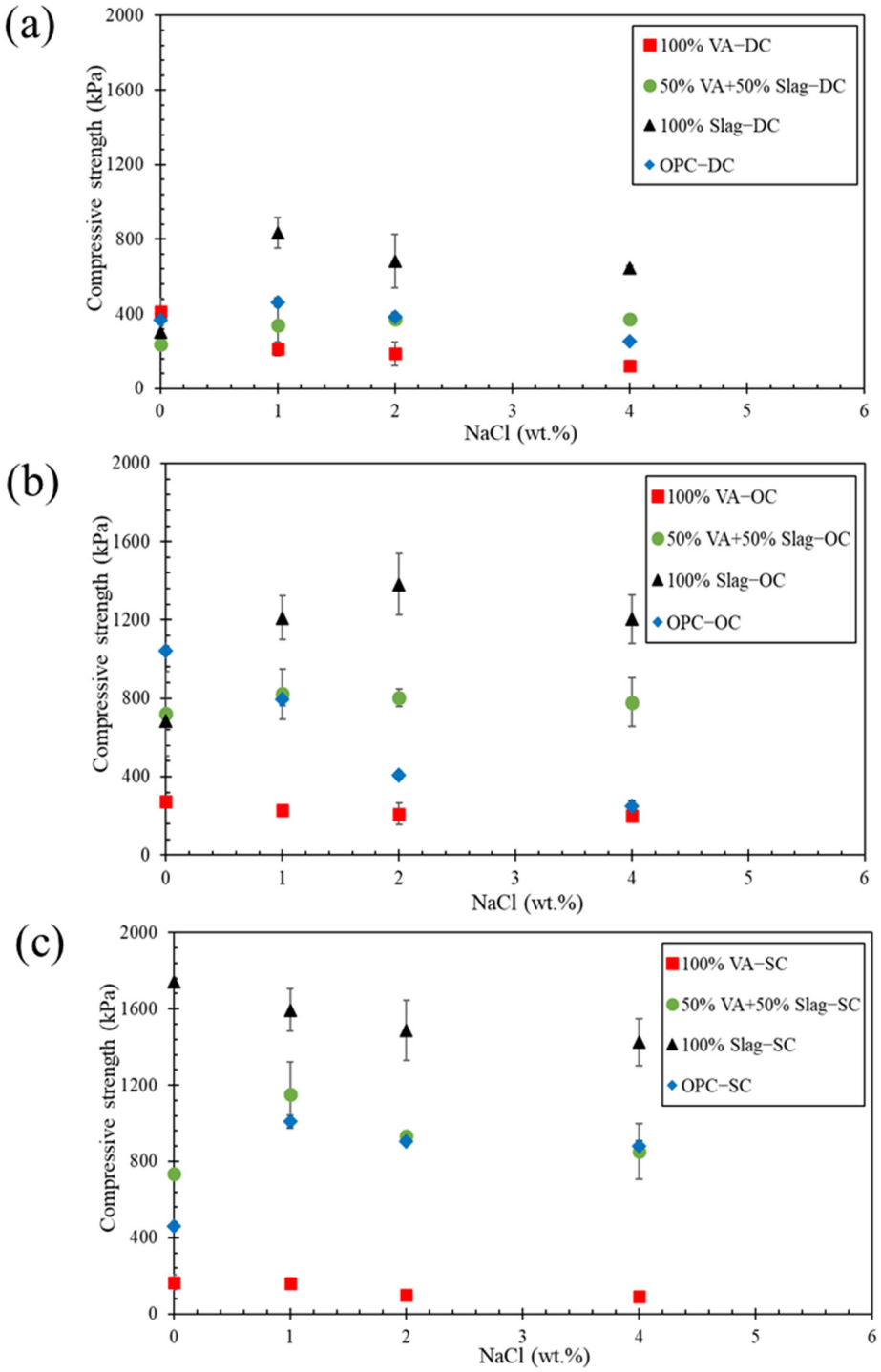

Figure 8. Effect of NaCl addition on 90-day mechanical strength of alkali-activated and Portland-cement-stabilized soil samples at (**a**) DC, (**b**) OC, and (**c**) SC conditions.

The strength of soil samples stabilized with 100 wt.% volcanic ash had the highest value at the dry (DC) condition, and this value was lower at the wet (OC) condition, and finally, it reached its lowest value at the submerged (SC) condition. Low mechanical strength at the wet condition was due to the presence of high residual water in the sample and its very slow evaporation, which caused the alkalinity of the environment to rise slowly. Therefore, the mechanical strength of VA-based geopolymer at wet and submerged conditions was much lower than the dry condition. Because Si and Al leaching caused gel

formation and increased strength, this process did not occur well at wet and submerged conditions [37].

Curing conditions, including temperature and curing time, have a significant effect on the compressive strength of the samples. At low curing temperature, alkali-activated cements usually require a lengthy curing time to adequately dissolve the aluminosilicate elements and reach appropriate mechanical properties [58]. However, high curing temperature causes better and faster dissolution of aluminosilicates, and thus accelerates the geopolymerization process [40]. Meanwhile, curing at higher temperatures (without the presence of moisture) and for a long time causes the geopolymer structure to dehydrate the sample and results in excessive shrinkage of the sample, which ultimately reduces the compressive strength [38,46].

The mechanical properties of alkali-activated stabilized soil with 50 and 100 wt.% slag as well as Portland-cement-stabilized soil at the dry curing condition were fewer than the wet curing condition, and the strength of these stabilized soil samples in the wet condition was less than samples cured in the submerged condition. This is because the presence of water helps to accelerate the hydration reactions of the slag particles, which in turn increases the strength of the slag-containing samples over time.

Sandy and sand–silty beaches of seas and oceans have the potential of liquefaction in the event of an earthquake. Therefore, the use of chemical soil improvement methods is one of the regular methods for soil improvement in these areas [7]. Considering the chemical reactions between cementitious materials and chloride ions, it is very important to choose the type of cement as well as the appropriate type of additive in order to reduce the destructive effects of chlorine ions in soil improvement projects.

3.2. Microstructural Analysis

3.2.1. XRD Analysis

Figure 9 shows XRD patterns of alkali-activated cement-stabilized soil specimens at DC and SC conditions.

Generally, the main peaks observed in the alkali-activated volcanic-ash-stabilized soil samples (Figure 9a) correspond to the main peaks in volcanic ash and untreated soil. Alkali activation of volcanic ash led to the formation of sodium aluminosilicate gel (N-A-S-H) and the Ca-Chabazite phase [3,27,59]. The addition of sodium chloride to soil samples under both dry (DC) and submerged curing (SC) conditions did not change the crystalline structure but changed the peak intensity of the N-A-S-H gel. Previous studies have shown that N-A-S-H gel has a significant capacity for chloride ion surface adsorption [3].

In alkali-activated slag-stabilized soil samples (Figure 9b), the simultaneous formation of N-A-S-H and C-A-S-H phases leads to the formation of (N, C)-A-S-H phase, which has a very dense mechanical structure that leads to an increase in sample strength [27,38]. In addition, the formation of calcium silicate hydrate (C-S-H) gel can be observed in samples containing slag similar to previous research [60,61].

The (N, C)-A-S-H and C-S-H gels are clearly visible in alkali-activated VA/slag-stabilized soil samples (Figure 9c). The mechanism of action of these gels is to fill the cavities formed in the geopolymer matrix. In other words, filling the gap between the reacted and unreacted particles resulted in forming a denser structure of the samples [62,63]. High-calcium precursors (such as slag) played a significant role in the formation of C-A-S-H gel and increased the microstructure density of the sample [64]. As a result, the strength of the samples dramatically improved as the amount of slag increased, especially during SC conditions because in the presence of sufficient water, the formation of C-S-H and C-A-S-H gels in samples containing slag will be very probable. In stabilized soil samples containing slag and volcanic ash, the surface adsorption mechanism of chloride ion by N-A-S-H gel and the chemical encapsulation mechanism of chloride ion by (N, C)-A-S-H and C-S-H gels occurred simultaneously [65].

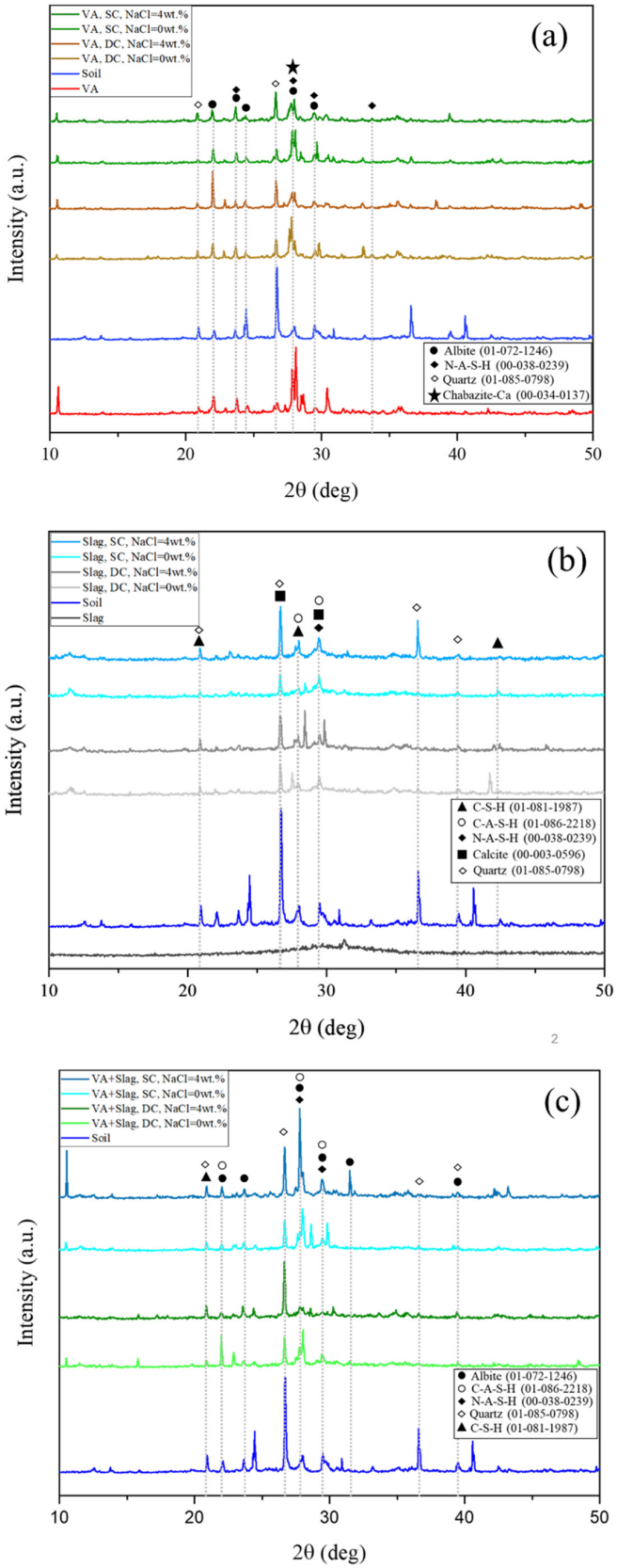

Figure 9. XRD patterns of (**a**) alkali-activated volcanic-ash-stabilized soil specimens, (**b**) alkali-activated slag-stabilized soil specimens, and (**c**) alkali-activated volcanic ash and slag stabilized soil specimens at DC and SC conditions (90-day curing).

In SC specimens, the samples were soaked in water during the curing time. So, NaCl was almost leached into the water and not detected in XRD patterns. However, in DC specimens, NaCl was probably converted to other compounds which may be a reason for not being detected in XRD patterns [3,66].

3.2.2. FTIR Analysis

Figure 10 presents the FTIR spectra of alkali-activated cement-stabilized soil specimens at DC and SC conditions.

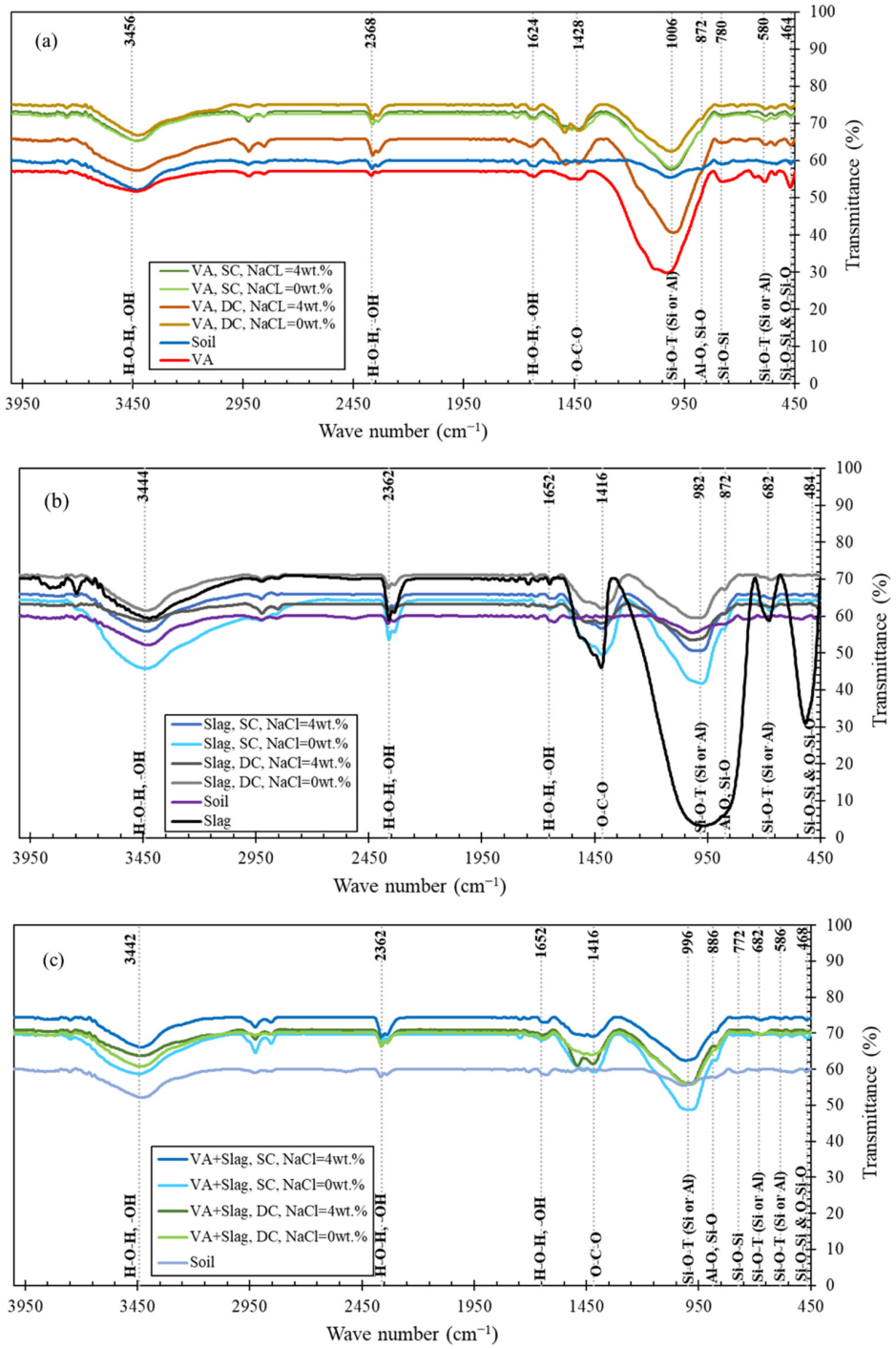

Figure 10. FTIR spectra of (**a**) alkali-activated volcanic-ash-stabilized soil specimens, (**b**) alkali-activated slag-stabilized soil specimens, and (**c**) alkali-activated volcanic ash and slag stabilized soil specimens at DC and SC conditions (90-day curing).

Aluminosilicate bonds in phases N-A-S-H and C-A-S-H are related to the bands detected in the range of 450–1100 cm^{-1} [59].

In alkali-activated volcanic-ash-stabilized soil samples (Figure 10a), the addition of sodium chloride at DC condition deepened the peak of the waves and reduced the wave transmission in the range of 450–1100 cm^{-1} in comparison with chloride-free specimens. This can illustrate a higher compaction of N-A-S-H gel matrix and prevent the strength reduction at the DC condition, while in submerged curing (SC) conditions, the FTIR spectrum of samples with and without sodium chloride overlaps. It is assumed that it is probably due to the leaching of sodium chloride from inside the sample to the water around the sample. This can be due to the physical (surface) adsorption of chloride ions by N-A-S-H gel [3]. Therefore, chloride ions leaching in the presence of water caused porosity in the structure of soil samples and reduced the mechanical properties.

Bands in the 550–750 cm^{-1} range were seen in all samples, representing the existence of an amorphous aluminosilicate structure [67].

Bands in the 1600–1700 cm^{-1} range indicated structural water and the bands in the 2300–2400 cm^{-1} and 3000–3500 cm^{-1} ranges indicated residual water, respectively [38,59].

The peak intensity was higher in the range of 1600–1700 cm^{-1}, as well as in the ranges of 2300–2400 cm^{-1} and 3000–3500 cm^{-1} at DC conditions in alkali-activated volcanic-ash-stabilized soil samples (Figure 10a), which may be attributed to the better generation of VA-based geopolymer gel. In other words, a stronger O-H bond results in increased water absorption, which in turn leads to higher environmental alkalinity.

In alkali-activated slag-stabilized soil samples (Figure 10b), the peak intensity in the range of 450–1100 cm^{-1} was higher in the submerged condition than in dry condition. Because the presence of moisture caused more density of C-S-H and C-A-S-H gels, this led to an increase in the strength of the samples [38].

Previous studies showed that the O-H bond formed between 3000 and 3500 cm^{-1} may be related to the C-S-H bond, indicating that the strength of the bond increases with peak strength [67,68].

In alkali-activated VA–slag-stabilized soil samples (Figure 10c), the FTIR spectrum of samples with and without sodium chloride overlaps at the DC condition. Meanwhile, as in alkali-activated slag-stabilized soil samples, the peak intensity in the range of 450–1100 cm^{-1}, as well as in the range of 1600–1700 cm^{-1}, 2300–2400 cm^{-1}, and 3000–3500 cm^{-1} in samples without sodium chloride, was higher than sodium chloride containing samples at the SC condition, which indicates the negative effect of sodium chloride on the mechanical properties of the samples.

Peak intensities of 1410–1440 cm^{-1} were higher in alkali-activated stabilized soil samples with 50 and 100 wt.% slag than in samples containing volcanic ash. The alkali metal hydroxides in alkali-activated cement react with the CO_2 in the air to generate carbonates, which are associated to the 1410–1440 cm^{-1} range peaks [67,68].

The Al-O or Si-O bond is equivalent to the bonds in the 860–890 cm^{-1} range [67,68]. This bond was easier to see in the slag-based specimens, and it may be the cause of the strength development in the alkali-activated slag-stabilized soil samples.

3.2.3. SEM–EDS Mapping Analysis

Figures 11–13 show the SEM images of alkali-activated cement-stabilized soil specimens at DC and SC conditions. Changes in the microscopic structure of alkali-activated cement-stabilized soil samples containing 100 wt.% volcanic ash, 100 wt.% slag, and 50 wt.% volcanic ash and 50 wt.% slag are observed in Figures 11–13, respectively. Samples were studied in two cases without sodium chloride and containing sodium chloride at dry (DC) and submerged (SC) conditions.

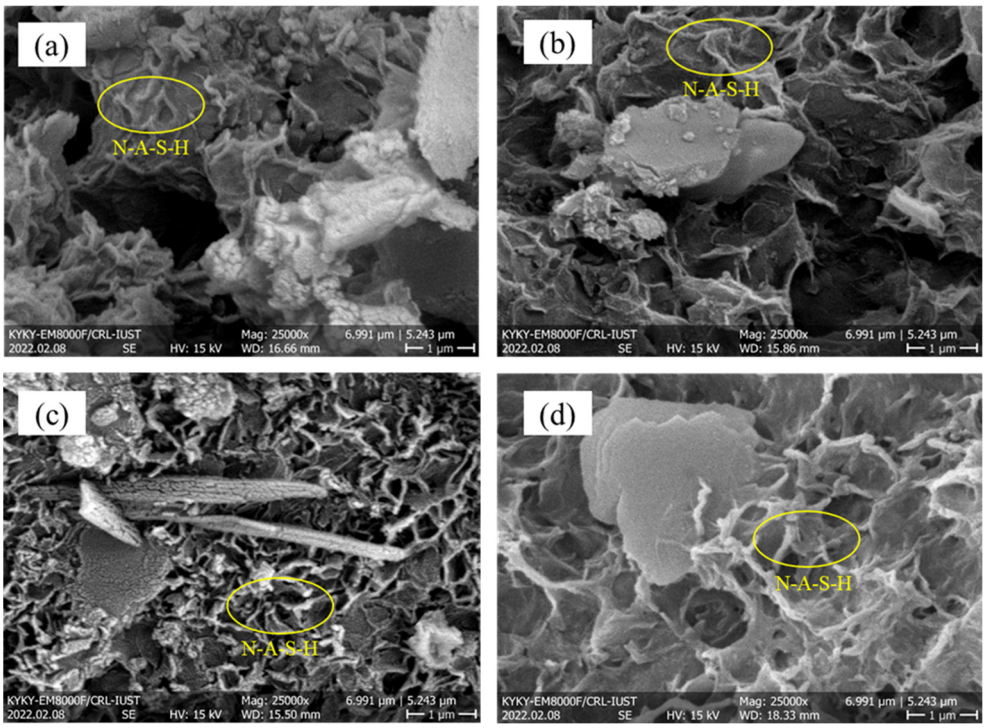

Figure 11. The SEM images of the alkali-activated volcanic-ash-stabilized soil specimens at DC condition (90-day curing), (**a**) without sodium chloride, (**b**) with 4 wt.% sodium chloride and SC condition (90-day curing), (**c**) without sodium chloride, and (**d**) with 4 wt.% sodium chloride.

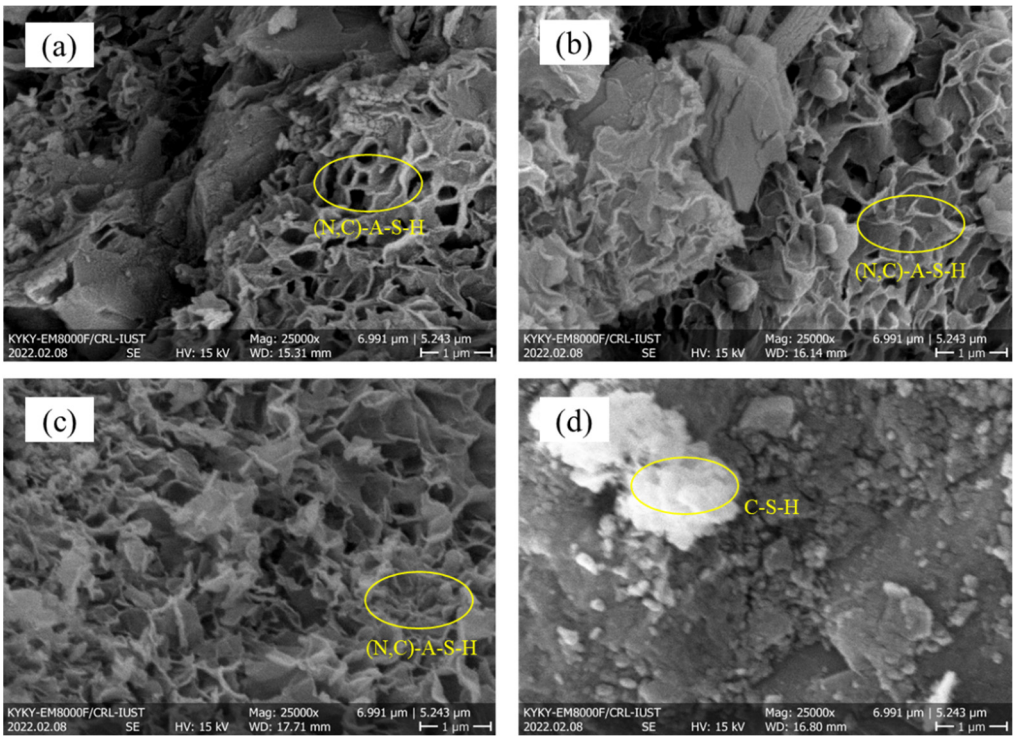

Figure 12. The SEM images of the alkali-activated slag-stabilized soil specimens at DC condition (90-day curing), (**a**) without sodium chloride, (**b**) with 4 wt.% sodium chloride and SC condition (90-day curing), (**c**) without sodium chloride, and (**d**) with 4 wt.% sodium chloride.

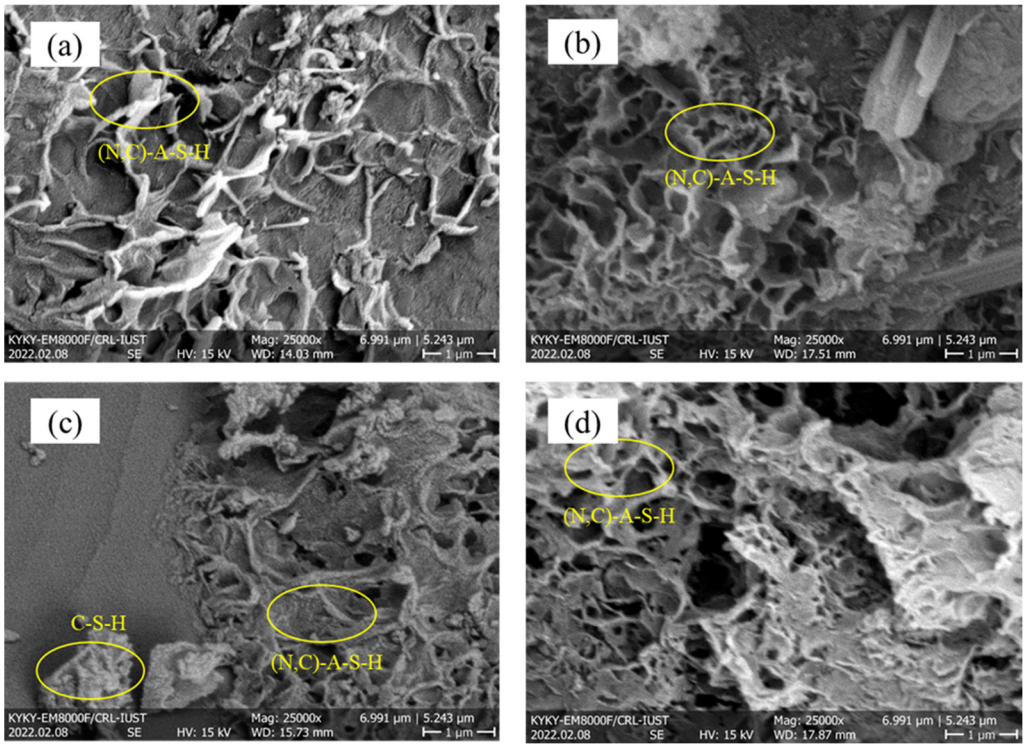

Figure 13. The SEM images of the alkali-activated volcanic ash and slag stabilized soil specimens at DC condition (90-day curing), (**a**) without sodium chloride, (**b**) with 4 wt.% sodium chloride and SC condition (90-day curing), (**c**) without sodium chloride, and (**d**) with 4 wt.% sodium chloride.

Generally, propagation of alkali activation products through the voids of sand particles results in a dense structure and mechanical strength development.

In alkali-activated volcanic-ash-stabilized soil samples (Figure 11), the density of N-A-S-H geopolymer gel in specimens with sodium chloride was higher than specimens without sodium chloride, which was consistent with the results of XRD and FTIR tests.

In alkali-activated slag-stabilized soil samples (Figure 12), the density of (N, C)-A-S-H and C-S-H gels were higher at the submerged curing (SC) condition than at the dry curing (DC) condition, which was consistent with the FTIR results. In other words, the structural density of these samples at the submerged condition was higher than the dry condition, which led to the strength development of the specimens at the submerged condition.

In all three alkali-activated cement mix designs and at submerged curing conditions, the addition of sodium chloride changed the shape, structure, and morphology of the gels formed [59].

In general, with the addition of slag and the formation of C-S-H as well as C-A-S-H gels, the porosity of the samples decreased [38]. Therefore, the mechanical properties of the samples increased compared with the samples without slag.

Figure 14a–c shows the EDS results of alkali-activated cement-stabilized soil samples containing 100 wt.% volcanic ash, 100 wt.% slag, and 50 wt.% volcanic ash and 50 wt.% slag, respectively. The production of N-A-S-H, (N,C)-A-S-H gel, and C-S-H gels in the presence of sodium, calcium, and aluminum were reported by the previous literature [38,59].

According to the co-existence of calcium and silicon elements in marked areas (white ovals in Figure 15a) in alkali-activated slag-stabilized soil samples, the possibility of C-S-H gel is very high [38]. Furthermore, the relatively uniform distribution of chloride ion (black ovals in Figure 15b) in a sample containing sodium chloride indicated its adsorption by cementitious gels.

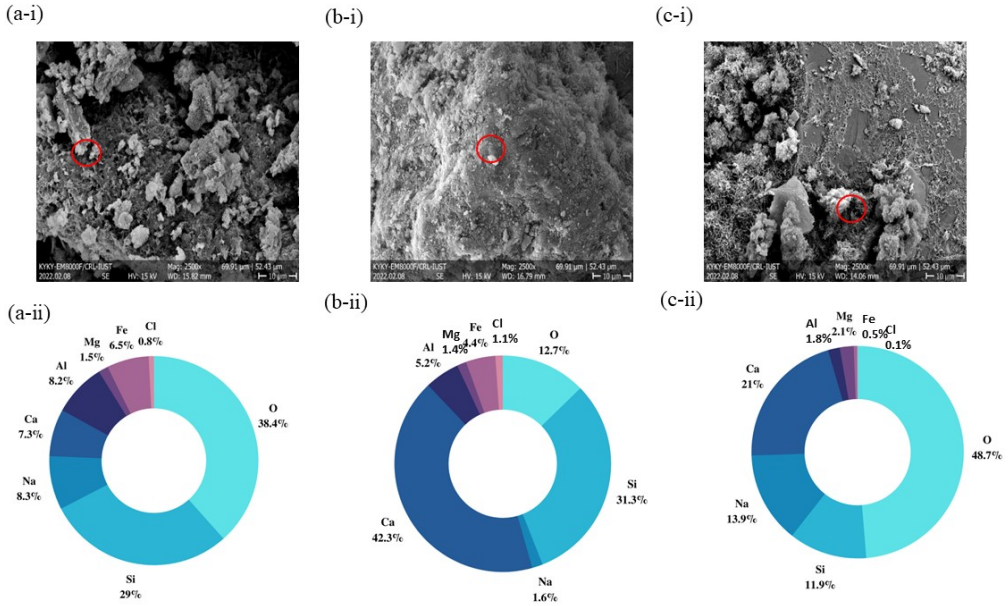

Figure 14. EDS results of the (**a**-i,**a**-ii) alkali-activated volcanic ash, (**b**-i,**b**-ii) alkali-activated slag, and (**c**-i,**c**-ii) alkali-activated volcanic ash and slag stabilized soil specimens at DC condition (90-day curing) with 4 wt.% sodium chloride.

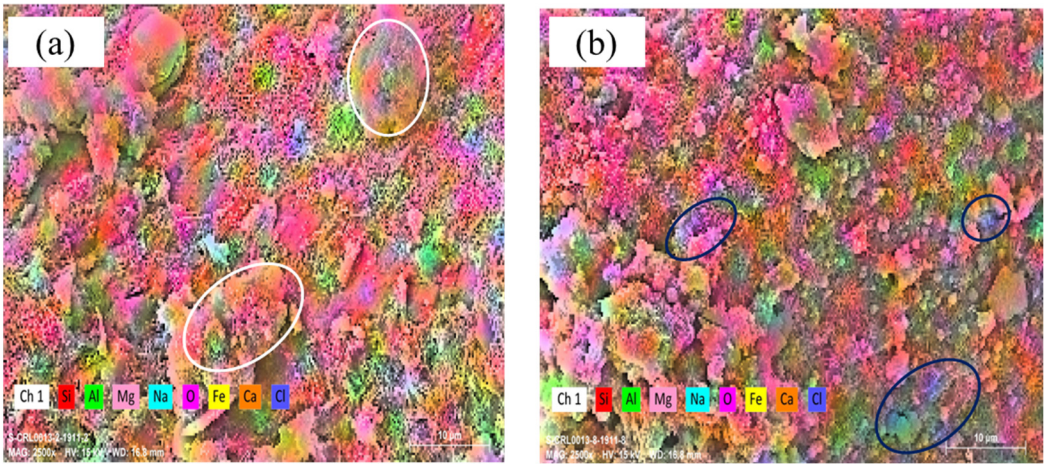

Figure 15. Elemental mapping analysis of the alkali-activated slag-stabilized soil specimen at DC condition (90-day curing) (**a**) without sodium chloride and (**b**) with 4 wt.% sodium chloride.

4. Conclusions

This paper investigated the effect of NaCl on the microstructural and mechanical properties of alkali-activated/Portland-cement-stabilized sandy soil. The results reported in this research lead to the following conclusions.

- In soil samples stabilized with alkali-activated volcanic ash, adding sodium chloride from 0 to 4 wt.% decreased the long-term (90 days) strength up to 70% in all three curing conditions. Meanwhile, the strength of soil specimens stabilized with alkali-activated slag increased up to 244% when the sodium chloride content was raised by 1 wt.%, and adding more sodium chloride content (up to 4 wt.%) had a nuanced effect on the strength under all curing conditions.
- In soil samples stabilized with alkali-activated volcanic ash, the density of N-A-S-H geopolymer gel in specimens with sodium chloride was higher than specimens without sodium chloride, which was consistent with the results of the XRD and FTIR tests.

- In stabilized soil samples containing slag and volcanic ash, the surface adsorption mechanism of chloride ion by N-A-S-H gel and the chemical encapsulation mechanism of chloride ion by (N, C)-A-S-H and C-S-H gels occurred simultaneously.
- It can be concluded that alkali-activated slag cement can be a sustainable alternative to Portland cement for saline soil stabilization.

Author Contributions: Conceptualization, P.G.; methodology, P.G.; software, P.G.; validation, H.R.R. and A.A.J.; formal analysis, P.G.; investigation, P.G.; resources, H.R.R. and A.A.J.; data curation, P.G.; writing—original draft preparation, P.G.; writing—review and editing, H.R.R. and A.A.J.; visualization, P.G.; supervision, H.R.R. and A.A.J.; project administration, H.R.R. and A.A.J.; funding acquisition, H.R.R. and A.A.J. All authors have read and agreed to the published version of the manuscript.

Funding: The APC was funded by the University of Exeter.

Data Availability Statement: Data that support the findings of this study are available from the corresponding author upon reasonable request.

Acknowledgments: The authors would like to appreciate Iran's National Elites Foundation and European Union's Horizon 2020 research and innovation program under the Marie Sklodowska-Curie grant agreement No 778120. This study was supported by MatSoil Company (No. 02A/2022).

Conflicts of Interest: The authors declare no conflict of interest.

References

1. Cuisinier, O.; Le Borgne, T.; Deneele, D.; Masrouri, F. Quantification of the effects of nitrates, phosphates and chlorides on soil stabilization with lime and cement. *Eng. Geol.* **2011**, *117*, 229–235. [CrossRef]
2. Ying, Z.; Cui, Y.-J.; Benahmed, N.; Duc, M. Salinity assessment for salted soil considering both dissolved and precipitated salts. *Geotech. Test. J.* **2020**, *44*, 9-p. [CrossRef]
3. Chen, Z.; Ye, H. Influence of metakaolin and limestone on chloride binding of slag activated by mixed magnesium oxide and sodium hydroxide. *Cem. Concr. Compos.* **2021**, *127*, 104397. [CrossRef]
4. Ghavami, S.; Jahanbakhsh, H.; Saeedi Azizkandi, A.; Moghadas Nejad, F. Influence of sodium chloride on cement kiln dust-treated clayey soil: Strength properties, cost analysis, and environmental impact. *Environ. Dev. Sustain.* **2021**, *23*, 683–702. [CrossRef]
5. Mishra, P.N.; Scheuermann, A.; Bore, T.; Li, L. Salinity effects on soil shrinkage characteristic curves of fine-grained geomaterials. *J. Rock Mech. Geotech. Eng.* **2019**, *11*, 181–191. [CrossRef]
6. Armistead, S.J.; Smith, C.C.; Staniland, S.S. Sustainable biopolymer soil stabilization in saline rich, arid conditions: A 'micro to macro'approach. *Sci. Rep.* **2022**, *12*, 2880. [CrossRef] [PubMed]
7. Khoshsirat, V.; Bayesteh, H.; Sharifi, M. Effect of high salinity in grout on the performance of cement-stabilized marine clay. *Constr. Build. Mater.* **2019**, *217*, 93–107. [CrossRef]
8. Barman, D.; Dash, S.K. Stabilization of expansive soils using chemical additives: A review. *J. Rock Mech. Geotech. Eng.* **2022**, *14*, 1319–1342. [CrossRef]
9. Liu, J.; Zha, F.; Xu, L.; Yang, C.; Chu, C.; Tan, X. Effect of chloride attack on strength and leaching properties of solidified/stabilized heavy metal contaminated soils. *Eng. Geol.* **2018**, *246*, 28–35. [CrossRef]
10. Ying, Z.; Cui, Y.-J.; Benahmed, N.; Duc, M. Salinity effect on the compaction behaviour, matric suction, stiffness and microstructure of a silty soil. *J. Rock Mech. Geotech. Eng.* **2021**, *13*, 855–863. [CrossRef]
11. Islam, M.M.; Islam, M.S.; Mondal, B.C.; Das, A. Strength behavior of mortar using slag with cement in sea water environment. *J Civ Eng-IEB* **2009**, *37*, 111–122.
12. Kaushik, S.; Islam, S. Suitability of sea water for mixing structural concrete exposed to a marine environment. *Cem. Concr. Compos.* **1995**, *17*, 177–185. [CrossRef]
13. Qiao, C.; Suraneni, P.; Weiss, J. Damage in cement pastes exposed to NaCl solutions. *Constr. Build. Mater.* **2018**, *171*, 120–127. [CrossRef]
14. Xing, H.; Yang, X.; Xu, C.; Ye, G. Strength characteristics and mechanisms of salt-rich soil–cement. *Eng. Geol.* **2009**, *103*, 33–38. [CrossRef]
15. Zhang, D.; Cao, Z.; Fan, L.; Liu, S.; Liu, W. Evaluation of the influence of salt concentration on cement stabilized clay by electrical resistivity measurement method. *Eng. Geol.* **2014**, *170*, 80–88. [CrossRef]
16. Horpibulsuk, S.; Phojan, W.; Suddeepong, A.; Chinkulkijniwat, A.; Liu, M.D. Strength development in blended cement admixed saline clay. *Appl. Clay Sci.* **2012**, *55*, 44–52. [CrossRef]
17. Dingwen, Z.; Libin, F.; Songyu, L.; Yongfeng, D. Experimental investigation of unconfined compression strength and stiffness of cement treated salt-rich clay. *Mar. Georesources Geotechnol.* **2013**, *31*, 360–374. [CrossRef]

18. Cristelo, N.; Glendinning, S.; Miranda, T.; Oliveira, D.; Silva, R. Soil stabilisation using alkaline activation of fly ash for self compacting rammed earth construction. *Constr. Build. Mater.* **2012**, *36*, 727–735. [CrossRef]
19. Modmoltin, C.; Voottipruex, P. Influence of salts on strength of cement-treated clays. *Proc. Inst. Civ. Eng. -Ground Improv.* **2009**, *162*, 15–26. [CrossRef]
20. Shariatmadari, N.; Hasanzadehshooiili, H.; Ghadir, P.; Saeidi, F.; Moharami, F. Compressive strength of sandy soils stabilized with alkali-activated volcanic ash and slag. *J. Mater. Civ. Eng.* **2021**, *33*, 04021295. [CrossRef]
21. Araújo, N.; Corrêa-Silva, M.; Miranda, T.; Topa Gomes, A.; Castro, F.; Teixeira, T.; Cristelo, N. Unsaturated response of clayey soils stabilised with alkaline cements. *Molecules* **2020**, *25*, 2533. [CrossRef] [PubMed]
22. Žurinskas, D.; Vaičiukynienė, D.; Stelmokaitis, G.; Doroševas, V. Clayey Soil Strength Improvement by Using Alkali Activated Slag Reinforcing. *Minerals* **2020**, *10*, 1076. [CrossRef]
23. Mohebbi, H.R.; Javadi, A.A.; Saeedi Azizkandi, A. The Effects of Soil Porosity and Mix Design of Volcanic Ash-Based Geopolymer on the Surface Strength of Highly Wind Erodible Soils. *Minerals* **2022**, *12*, 984. [CrossRef]
24. Şahin, E.; Çiftçioğlu, M. Monetite promoting effect of NaCl on brushite cement setting kinetics. *J. Mater. Chem. B* **2013**, *1*, 2943–2950. [CrossRef] [PubMed]
25. Odeh, N.A.; Al-Rkaby, A.H. Strength, Durability, and Microstructures characterization of sustainable geopolymer improved clayey soil. *Case Stud. Constr. Mater.* **2022**, *16*, e00988. [CrossRef]
26. Ngo, T.-P.; Bui, Q.-B.; Phan, V.T.-A.; Tran, H.-B. Durability of geopolymer stabilised compacted earth exposed to wetting–drying cycles at different conditions of pH and salt. *Constr. Build. Mater.* **2022**, *329*, 127168. [CrossRef]
27. Samantasinghar, S.; Singh, S.P. Strength and Durability of Granular Soil Stabilized with FA-GGBS Geopolymer. *J. Mater. Civ. Eng.* **2021**, *33*, 06021003. [CrossRef]
28. *ASTM D2487-17e1*; Standard Practice for Classification of Soils for Engineering Purposes (Unified Soil Classification System). American Society for Testing and Materials (ASTM): West Conshohocken, PA, USA, 2017.
29. Konyushkova, M.; Alavipanah, S.; Heidari, A.; Kozlov, D.; Yu, M.; Semenkov, I. Spatial and seasonal salt translocation in the young soils at the coastal plains of the Caspian Sea. *Quat. Int.* **2021**, *590*, 15–25. [CrossRef]
30. *ASTM D422-63*; Standard Test Method for Particle-Size Analysis of Soils. American Society for Testing and Materials (ASTM): West Conshohocken, PA, USA, 2002.
31. *ASTM D7928-21e1*; Standard Test Method for Particle-Size Distribution (Gradation) of Fine-Grained Soils Using the Sedimentation (Hydrometer) Analysis. American Society for Testing and Materials (ASTM): West Conshohocken, PA, USA, 2021.
32. *ASTM D4253-16e1*; Standard Test Methods for Maximum Index Density and Unit Weight of Soils Using a Vibratory Table. American Society for Testing and Materials (ASTM): West Conshohocken, PA, USA, 2019.
33. *ASTM D4254-16*; Standard Test Methods for Minimum Index Density and Unit Weight of Soils and Calculation of Relative Density. American Society for Testing and Materials (ASTM): West Conshohocken, PA, USA, 2016.
34. *ASTM D854-14*; Standard Test Methods for Specific Gravity of Soil Solids by Water Pycnometer. American Society for Testing and Materials (ASTM): West Conshohocken, PA, USA, 2016.
35. Sun, J.; Huang, Y. Modeling the Simultaneous Effects of Particle Size and Porosity in Simulating Geo-Materials. *Materials* **2022**, *15*, 1576. [CrossRef]
36. *ASTM D2166-16*; Standard Test Method for Unconfined Compressive Strength of Cohesive Soil. American Society for Testing and Materials (ASTM): West Conshohocken, PA, USA, 2016.
37. Ghadir, P.; Zamanian, M.; Mahbubi-Motlagh, N.; Saberian, M.; Li, J.; Ranjbar, N. Shear strength and life cycle assessment of volcanic ash-based geopolymer and cement stabilized soil: A comparative study. *Transp. Geotech.* **2021**, *31*, 100639. [CrossRef]
38. Miraki, H.; Shariatmadari, N.; Ghadir, P.; Jahandari, S.; Tao, Z.; Siddique, R. Clayey soil stabilization using alkali-activated volcanic ash and slag. *J. Rock Mech. Geotech. Eng.* **2021**, *14*, 576–591. [CrossRef]
39. Van Deventer, J.; Provis, J.; Duxson, P.; Lukey, G. Reaction mechanisms in the geopolymeric conversion of inorganic waste to useful products. *J. Hazard. Mater.* **2007**, *139*, 506–513. [CrossRef] [PubMed]
40. Ghadir, P.; Ranjbar, N. Clayey soil stabilization using geopolymer and Portland cement. *Constr. Build. Mater.* **2018**, *188*, 361–371. [CrossRef]
41. Kuenzel, C.; Vandeperre, L.J.; Donatello, S.; Boccaccini, A.R.; Cheeseman, C. Ambient temperature drying shrinkage and cracking in metakaolin-based geopolymers. *J. Am. Ceram. Soc.* **2012**, *95*, 3270–3277. [CrossRef]
42. Ranjbar, N.; Mehrali, M.; Alengaram, U.J.; Metselaar, H.S.C.; Jumaat, M.Z. Compressive strength and microstructural analysis of fly ash/palm oil fuel ash based geopolymer mortar under elevated temperatures. *Constr. Build. Mater.* **2014**, *65*, 114–121. [CrossRef]
43. Pourakbar, S.; Huat, B.B.; Asadi, A.; Fasihnikoutalab, M.H. Model study of alkali-activated waste binder for soil stabilization. *Int. J. Geosynth. Ground Eng.* **2016**, *2*, 35. [CrossRef]
44. Xu, H.; van Deventer, J.S. The effect of alkali metals on the formation of geopolymeric gels from alkali-feldspars. *Colloids Surf. A: Physicochem. Eng. Asp.* **2003**, *216*, 27–44. [CrossRef]
45. Chi, M. Effects of dosage of alkali-activated solution and curing conditions on the properties and durability of alkali-activated slag concrete. *Constr. Build. Mater.* **2012**, *35*, 240–245. [CrossRef]
46. Mayhoub, O.A.; Mohsen, A.; Alharbi, Y.R.; Abadel, A.A.; Habib, A.; Kohail, M. Effect of curing regimes on chloride binding capacity of geopolymer. *Ain Shams Eng. J.* **2021**, *12*, 3659–3668. [CrossRef]

47. Ranjbar, N.; Mehrali, M.; Maheri, M.R.; Mehrali, M. Hot-pressed geopolymer. *Cem. Concr. Res.* **2017**, *100*, 14–22. [CrossRef]
48. Aldaood, A.; Bouasker, M.; Al-Mukhtar, M. Impact of wetting–drying cycles on the microstructure and mechanical properties of lime-stabilized gypseous soils. *Eng. Geol.* **2014**, *174*, 11–21. [CrossRef]
49. Farnam, Y.; Dick, S.; Wiese, A.; Davis, J.; Bentz, D.; Weiss, J. The influence of calcium chloride deicing salt on phase changes and damage development in cementitious materials. *Cem. Concr. Compos.* **2015**, *64*, 1–15. [CrossRef] [PubMed]
50. Birnin-Yauri, U.; Glasser, F. Friedel's salt, $Ca_2Al(OH)_6(Cl, OH)\cdot 2H_2O$: Its solid solutions and their role in chloride binding. *Cem. Concr. Res.* **1998**, *28*, 1713–1723. [CrossRef]
51. De Weerdt, K.; Orsáková, D.; Geiker, M.R. The impact of sulphate and magnesium on chloride binding in Portland cement paste. *Cem. Concr. Res.* **2014**, *65*, 30–40. [CrossRef]
52. Hirao, H.; Yamada, K.; Takahashi, H.; Zibara, H. Chloride binding of cement estimated by binding isotherms of hydrates. *J. Adv. Concr. Technol.* **2005**, *3*, 77–84. [CrossRef]
53. Thomas, M.; Hooton, R.; Scott, A.; Zibara, H. The effect of supplementary cementitious materials on chloride binding in hardened cement paste. *Cem. Concr. Res.* **2012**, *42*, 1–7. [CrossRef]
54. Yoon, S.; Ha, J.; Chae, S.R.; Kilcoyne, D.A.; Jun, Y.; Oh, J.E.; Monteiro, P.J. Phase changes of monosulfoaluminate in NaCl aqueous solution. *Materials* **2016**, *9*, 401. [CrossRef]
55. Kayali, O.; Khan, M.; Ahmed, M.S. The role of hydrotalcite in chloride binding and corrosion protection in concretes with ground granulated blast furnace slag. *Cem. Concr. Compos.* **2012**, *34*, 936–945. [CrossRef]
56. Du, Y.-J.; Wei, M.-L.; Reddy, K.R.; Liu, Z.-P.; Jin, F. Effect of acid rain pH on leaching behavior of cement stabilized lead-contaminated soil. *J. Hazard. Mater.* **2014**, *271*, 131–140. [CrossRef]
57. Du, Y.-J.; Bo, Y.-L.; Jin, F.; Liu, C.-Y. Durability of reactive magnesia-activated slag-stabilized low plasticity clay subjected to drying–wetting cycle. *Eur. J. Environ. Civ. Eng.* **2016**, *20*, 215–230. [CrossRef]
58. Noushini, A.; Castel, A. The effect of heat-curing on transport properties of low-calcium fly ash-based geopolymer concrete. *Constr. Build. Mater.* **2016**, *112*, 464–477. [CrossRef]
59. Ghadir, P.; Razeghi, H.R. Effects of sodium chloride on the mechanical strength of alkali activated volcanic ash and slag pastes under room and elevated temperatures. *Constr. Build. Mater.* **2022**, *344*, 128113. [CrossRef]
60. Khan, M.; Kayali, O.; Troitzsch, U. Chloride binding capacity of hydrotalcite and the competition with carbonates in ground granulated blast furnace slag concrete. *Mater. Struct.* **2016**, *49*, 4609–4619. [CrossRef]
61. Song, H.-W.; Saraswathy, V. Studies on the corrosion resistance of reinforced steel in concrete with ground granulated blast-furnace slag—An overview. *J. Hazard. Mater.* **2006**, *138*, 226–233. [CrossRef]
62. Lee, N.; Jang, J.G.; Lee, H.-K. Shrinkage characteristics of alkali-activated fly ash/slag paste and mortar at early ages. *Cem. Concr. Compos.* **2014**, *53*, 239–248. [CrossRef]
63. Wang, W.-C.; Wang, H.-Y.; Lo, M.-H. The fresh and engineering properties of alkali activated slag as a function of fly ash replacement and alkali concentration. *Constr. Build. Mater.* **2015**, *84*, 224–229. [CrossRef]
64. Ding, Y.; Dai, J.-G.; Shi, C.-J. Mechanical properties of alkali-activated concrete: A state-of-the-art review. *Constr. Build. Mater.* **2016**, *127*, 68–79. [CrossRef]
65. Ke, X.; Bernal, S.A.; Provis, J.L. Chloride binding capacity of synthetic C-(A)-SH type gels in alkali-activated slag simulated pore solutions. In Proceedings of the 1st International Conference on Construction Materials for Sustainable Future, Zadar, Croatia, 19–21 April 2017.
66. Zhu, Y.; Wan, X.; Han, X.; Ren, J.; Luo, J.; Yu, Q. Solidification of chloride ions in alkali-activated slag. *Constr. Build. Mater.* **2022**, *320*, 126219. [CrossRef]
67. Li, F.; Liu, L.; Yang, Z.; Li, S. Physical and mechanical properties and micro characteristics of fly ash-based geopolymer paste incorporated with waste Granulated Blast Furnace Slag (GBFS) and functionalized Multi-Walled Carbon Nanotubes (MWCNTs). *J. Hazard. Mater.* **2020**, *401*, 123339. [CrossRef]
68. Zhang, P.; Muhammad, F.; Yu, L.; Xia, M.; Lin, H.; Huang, X.; Jiao, B.; Shiau, Y.; Li, D. Self-cementation solidification of heavy metals in lead-zinc smelting slag through alkali-activated materials. *Constr. Build. Mater.* **2020**, *249*, 118756. [CrossRef]